Human Lamina Cribrosa Insertion and Age

Ian A. Sigal,[1–3] *John G. Flanagan,*[4,5] *Kira L. Lathrop,*[1] *Inka Tertinegg,*[4] *and Richard Bilonick*[1,6]

Purpose. To test the hypothesis that in healthy human eyes the lamina cribrosa (LC) insertion into the pia mater increases with age.

Methods. The optic nerve heads (ONHs) of donor eyes fixed at either 5 or 50 mm Hg of IOP were sectioned, stained, and imaged under bright- and dark-field conditions. A 3-dimensional (3D) model of each ONH was reconstructed. From the 3D models we measured the area of LC insertion into the peripapillary scleral flange and into the pia, and computed the total area of insertion and fraction of LC inserting into the pia. Linear mixed effect models were used to determine if the measurements were associated with age or IOP.

Results. We analyzed 21 eyes from 11 individuals between 47 and 91 years old. The LC inserted into the pia in all eyes. The fraction of LC inserting into the pia (2.2%–29.6%) had a significant decrease with age ($P = 0.049$), which resulted from a nonsignificant increase in the total area of LC insertion ($P = 0.41$) and a nonsignificant decrease in the area of LC insertion into the pia ($P = 0.55$). None of the measures was associated with fixation IOP (P values 0.44–0.81). Differences between fellow eyes were smaller than differences between unrelated eyes.

Conclusions. The LC insertion into the pia mater is common in middle-aged and older eyes, and does not increase with age. The biomechanical and vascular implications of the LC insertion into the pia mater are not well understood and should be investigated further. (*Invest Ophthalmol Vis Sci.* 2012;53:6870–6879) DOI:10.1167/iovs.12-9890

Loss of vision in glaucoma is due to damage to retinal ganglion cell axons responsible for transmitting information from the retina to the visual centers in the brain.[1,2] Evidence shows that axonal damage occurs at the level of the lamina cribrosa (LC), a specialized structure in the optic nerve head (ONH).[1–4] It is therefore of interest in glaucoma to understand the anatomy of the LC, and how it changes with aging and disease. The periphery of the LC is of particular importance from vascular and biomechanical perspectives, because the forces and deformations transmitted to the LC by the surrounding load-bearing tissues and scleral canal play a key role in the biomechanical robustness of the LC and sensitivity to elevated IOP.[1,2,5–8] In addition, much of the perfusion of the tissues within the LC, including the retinal ganglion cell axon bundles, is believed to be through microvessels and capillaries from the short posterior ciliary arteries, which enter the scleral canal from the periphery at the level of the LC insertion.[9–14]

We have shown that in ostensibly healthy humans between 70 and 91 years of age the LC often inserts partially into the pia mater and not only into the sclera.[15] A recent study reported that the LCs of young ostensibly healthy monkeys did not insert into the pia mater.[16] The question thus arises as to whether in humans the extent of LC insertion into the pia mater increases with aging. Our goal was to measure the LC insertion into the sclera and pia mater in healthy human donor eyes, and test the hypothesis that the LC insertion into the pia mater increases with age.

Methods

Eye Preparation

Donor eyes were obtained from the Eye Bank of Canada and processed in accordance with the provisions of the Declaration of Helsinki for research involving human tissue. A full description of the histologic techniques has been presented elsewhere.[15,17,18] Briefly, the eyes were placed in a custom chamber filled with physiologic saline maintained at 37°. Intraocular pressure was set by adjusting the level of saline in a reservoir connected to a cannula inserted into the eyes. IOP was then set to either 5 or 50 mm Hg above chamber pressure, and after equilibration for 15 minutes, the eyes were perfusion fixed by rapidly exchanging the isotonic saline with 2.5% paraformaldehyde/2.5% glutaraldehyde in Sorenson's phosphate buffer while maintaining IOP for 24 hours. When a pair of eyes was available, one eye was chosen randomly to be fixed and reconstructed at 5 mm Hg, whereas the contralateral eye was processed at 50 mm Hg.

Section Preparation and Imaging

After fixation, the ONH and peripapillary sclera were dissected free from the eye, dehydrated in a series of ethanols, and embedded in JB-4 plastic using a special mold that allowed the placement of tensioned collagen sutures for use as fiducial markers. Sagittal serial sections 2 μm thick were cut across the entire ONH at right angles to the axes of the fiducial markers. Sections at intervals of approximately 100 μm were photographed under dark field illumination (Leica MZ6, Heerbrugg, Switzerland) using a Nikon Coolpix 990 digital camera (2048 × 1536 pixels, 8 RGB bits per channel per pixel; Nikon, Tokyo, Japan) ensuring uniform sample illumination and nonsaturation of the brightest image regions (typically the sclera). Sections were then stained with

From the [1]Department of Ophthalmology, UPMC Eye Center, Eye and Ear Institute, Ophthalmology and Visual Science Research Center, University of Pittsburgh School of Medicine, Pittsburgh, Pennsylvania; the [2]McGowan Institute for Regenerative Science, University of Pittsburgh School of Medicine, Pittsburgh, Pennsylvania; the [3]Department of Bioengineering, Swanson School of Engineering, University of Pittsburgh, Pittsburgh, Pennsylvania, the [6]Department of Biostatistics, Graduate School of Public Health, University of Pittsburgh, Pittsburgh, Pennsylvania; the [4]Department of Ophthalmology and Vision Sciences, University of Toronto, Toronto, Ontario, Canada; and the [5]School of Optometry and Vision Science, University of Waterloo, Waterloo, Ontario, Canada.

Supported in part by National Institutes of Health Grant P30-EY008098 (Bethesda, Maryland); Eye and Ear Foundation (Pittsburgh, Pennsylvania); and unrestricted grants from Research to Prevent Blindness (New York, New York).

Submitted for publication March 20, 2012; revised August 10, 2012; accepted August 25, 2012.

Disclosure: **I.A. Sigal**, None; **J.G. Flanagan**, None; **K.L. Lathrop**, None; **I. Tertinegg**, None; **R. Bilonick**, None

Corresponding author: Ian A. Sigal, Ocular Biomechanics Laboratory, Department of Ophthalmology, UPMC Eye Center, University of Pittsburgh, 203 Lothrop Street, Rm. 930, Pittsburgh PA 15213; sigalia@upmc.edu.

Investigative Ophthalmology & Visual Science, October 2012, Vol. 53, No. 11

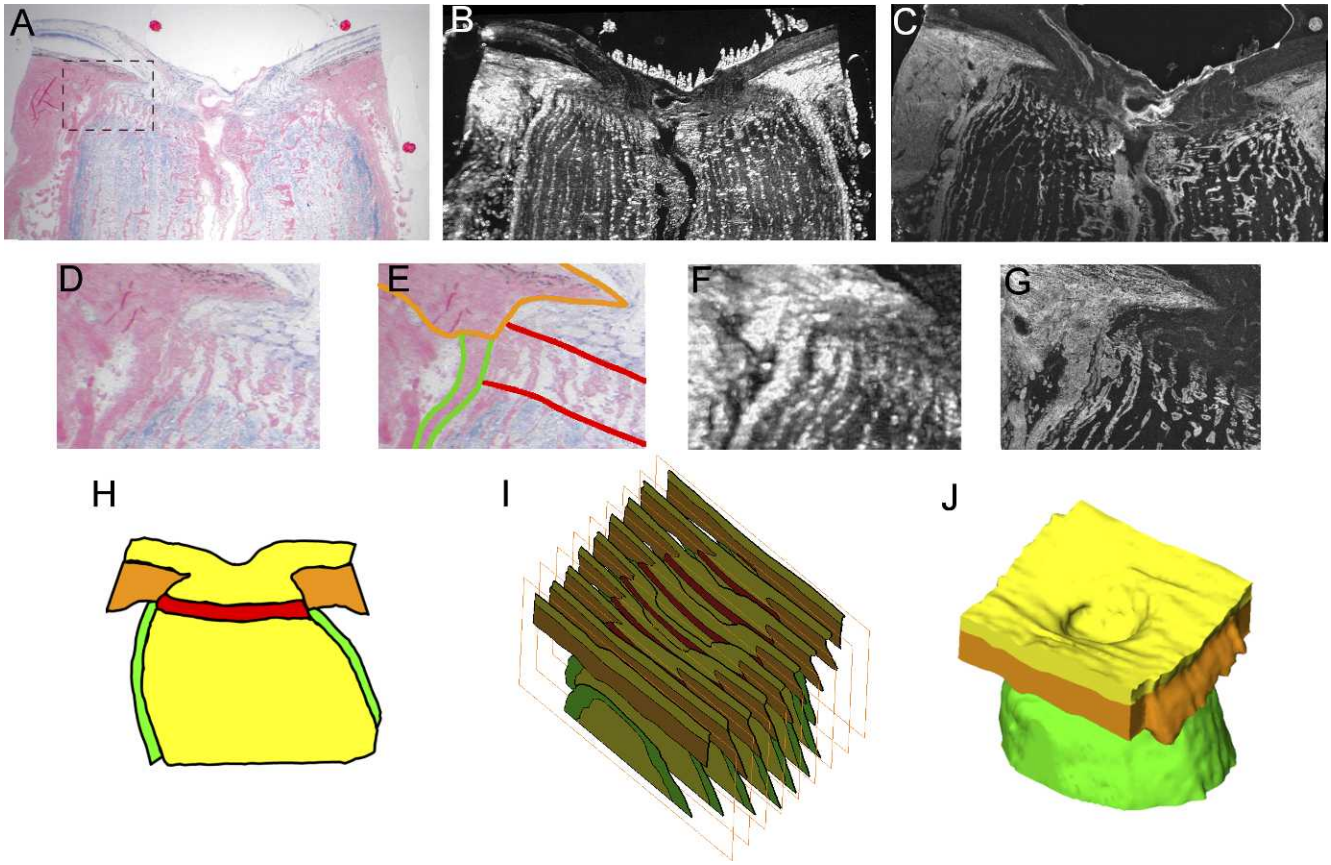

Figure 1. Example of lamina cribrosa partially inserting into the pia mater. Images of a superior-inferior section of the eye from Donor 5 (**A–G**). A combination of bright-field (**A**) and dark-field (**B**) images of dual-stained sections was used for tissue identification (segmentation [**E**]). The large discs (**A**, **B**) are fiducial markers inserted before embedding and sectioning, and used to align and unwarp the images. A confocal image confirms the collagen structures at higher resolution (**C**). The panels on the *middle row* are zoomed views of the region marked in (**A**) of either the bright-field (**D**, **E**), dark-field (**F**), or confocal (**G**) images. (**E**) Outlines of the lamina cribrosa (*red*), sclera (*orange*), and pia mater (*green*). The section is slightly temporal from the center of the scleral canal, which may explain the white ellipses on the prelaminar neural tissue, likely RGC axonal bundles sectioned at an angle. Note that the segmentations were done in 3D following the process described in detail in the text, not from a single slide (**H**). A stack of sections (**I**) then was used to reconstruct the 3D geometry of the specimen (**J**). Note also the thicker (**D**, **G**) and brighter (**F**) pia mater in the region of lamina insertion compared to pia mater further from the lamina.

picrosirius red to identify collagen, and solochrome cyanin to identify myelin, nuclei, and blood cells, and photographed under bright field illumination using the same procedure. Fluorescence images were acquired (Olympus Fluoview laser scanning confocal microscope; Olympus, Tokyo, Japan) to confirm the edges of the collagen structures at higher resolution (1.24 μm/pixel).

Image Processing

Images were aligned and unwarped to correct the deformations that occurred during the sectioning process (Fig. 1, top row) using a custom modified version of TPSSuper (F. James Rohlf, SUNY, Stony Brook, NY) based on the known fiducial marker positions as cast into the histologic block during the embedding procedure. This method avoided the use of anatomic features for alignment, which can lead to artifacts.[15,17] Image magnifications were calibrated using measurements of inter-fiducial distances taken before sectioning.

Tissue Segmentation (Delineation)

The digital sections were segmented manually to define five tissue regions: sclera, LC, prelaminar neural tissue, postlaminar neural tissue (including the optic nerve), and pia mater (Fig. 1, middle row). We used the dark-field and bright-field images to different extents depending on the tissue being identified. The concurrent use of dark- and bright-field images for the same section improved the decisions made during reconstruction, since not all features of the geometry were visible equally in all imaging modalities. The sclera was dense and fibrous in the dark-field images, and in the bright-field images it had the most intense picrosirius staining. The pia mater also stained well for collagen, and was bright and amorphous in the dark-field images. The anterior boundary of the LC was defined by the termination of the laminar beams and the insertion points at the sclera, whereas the posterior boundary was defined by two features: the termination of solochrome cyanin staining, indicating a lack of myelination inside the LC,[4] and the "stacked plate" morphology of the connective tissues typical of the LC.[4,8,19–22] The vitreoretinal interface was distinguishable clearly, as were the boundaries where the ONH had been cut from the rest of the eye. To ensure consistency across all eyes, all the segmentations were checked and adjusted by a single observer (JGF).

Surfacing and Measurement

To generate 3-dimensional (3D) reconstructions the image stack was expanded by adding virtual sections between the ones obtained from the histology.[15,17] The new sections were cubic interpolations inserted evenly (~33 μm apart; i.e., two interpolated sections between a pair of original sections). The interpolated sections were then cleaned of artefacts of interpolation and smoothed in all three projections. Although interpolation did not add any new information, it simplified

the production of 3D geometries while preserving a physiologically reasonable morphology. A triangulated surface mesh enclosing the segmented tissue regions was generated using a generalized marching cubes algorithm. Segmentation, surfacing, and visualization were performed using commercial software (Amira Dev3.1; Visage Imaging, Richmond, Victoria, Australia).

From 3D surfaces we measured the area of LC insertion into the peripapillary scleral flange and pia, and from this computed the total LC insertion and the fraction of the total LC insertion that was into the pia. An example LC insertion is shown in Figure 1. We emphasize that all measures were taken from the full 3D structure of the reconstructed ONH tissues (see Supplementary Material and Supplementary Movie 1, available at http://www.iovs.org/lookup/suppl/doi:10.1167/iovs.12-9890/-/DCSupplemental).

Segmentation and Surfacing Quality Control

The whole ONH was segmented and reconstructed to ensure that the 3D structures analyzed were anatomically sound, limiting the artefacts due to tissue preparation and processing. As described in our previous reports, a crucial element of our reconstruction process was its iterative nature.[15,17] Small iterative refinements were made to the image alignment (translation and rotation) and segmentation to reduce irregularities, and ensure that the tissue regions and interfaces between them were anatomically plausible and topologically valid. For example, tissue surfaces had to be smooth, with no bumps, ripples, or waves, due to the discrete nature of the serial sections. Tissue regions in the 3D reconstructions had to match tissue labeling in the histologic sections. If small adjustments were required during the iterative process to satisfy quality requirements, changes in the segmentation were accepted only if they matched the histologic images. This meant that changes were made mostly to the interpolated sections, leaving the original sections unchanged.

Statistical Analysis

We analyzed the data using linear mixed effects models with random intercepts to determine if the measurements were associated with age or IOP. We checked for normality and homogeneity by visual inspections of plots of residuals against fitted values. Results were considered significant when $P < 0.05$. We used the intraclass correlation coefficient (ICC) to test whether differences in measurements between contralateral eyes were smaller than between unrelated eyes. When the measurements for contralateral eyes were identical the ICC = 1. Conversely, when they were unrelated ICC = 0. Data were analyzed statistically using the open R language and environment for statistical computing (Version 2.14.1; R Development Core Team[23]) and the R package lme4.[24]

Robustness of the Results

While analyzing the results, we noticed that Donor 7 was particularly young (47 years, 18 years less than the next youngest donor) and, therefore, that the measurements from this subject had high leverage on the statistical model. Thus, we tested the robustness of the results by repeating the analysis using several alternative tissue segmentations of the eyes of Donor 7. Specifically, we used segmentations by each of three different people (IT, JGF, and IAS), as well as with and without the manual corrections described above. The largest differences were due to the corrections made on the smoothness of interpolated sections near the nasal and temporal edges of the LC. We also repeated the analysis without the measurements on the eyes of Donor 7.

Results

Twenty-one ostensibly healthy eyes from 11 human donors aged 47 to 91 years (mean 76.05 years, SD 11.72 years) were obtained within 24 hours postmortem (Fig. 2). After processing, all four measurements were collected (Fig. 3) and analyzed (Fig. 4, Table). The LC inserted into the pia mater in all eyes (fraction of LC inserting into the pia ranging between 2.2% and 29.6%). The total area of LC insertion and of LC insertion into the sclera tended to increase with age, although the effects were not statistically significant ($P = 0.4092$ and 0.3052, respectively, see the table). The area of LC insertion into the pia had a negative tendency, which was not significant ($P = 0.5536$). Differences between fellow eyes were smaller than differences between unrelated eyes (ICC's between 0.53 and 0.79). None of the measures was associated with the level of IOP at fixation (P values 0.44–0.81).

The reconstructions with the alternate segmentations had slightly different areas of LC insertion, but the statistical models for the areas of LC insertion into the sclera, into the pia, and total insertion remained essentially unchanged. The model of the fraction of LC inserting into the pia mater, however, did change. Baseline reconstructions, which we believe are the most appropriate, had insertion fractions of 21% and 23% for the right and left eyes, respectively. With alternate segmentations, these fractions varied between 18% and 23% for the right

Table. Summary of the Measurements and Statistical Models

Measurements	Age	LC Insertion			Fraction of Total into Pia
		Sclera	Pia Mater	Total	
Mean	76.05 y	1.20 mm^2	0.17 mm^2	1.37 mm^2	11.9%
Median	79.00 y	1.00 mm^2	0.16 mm^2	1.13 mm^2	10.9%
SD	11.72 y	0.43 mm^2	0.15 mm^2	0.52 mm^2	7.1%
Minimum	47.00 y	0.65 mm^2	0.03 mm^2	0.69 mm^2	2.2%
Maximum	91.00 y	1.94 mm^2	0.69 mm^2	2.33 mm^2	29.6%
LME model (age)					
P	–	0.31	0.55	0.41	0.049
Slope	–	0.012 mm^2/y	−0.002 mm^2/y	0.012 mm^2/y	−0.317%/y
95% CI					
Minimum	–	−0.013 mm^2/y	−0.011 mm^2/y	−0.019 mm^2/y	−0.632%/y
Maximum	–	0.037 mm^2/y	0.006 mm^2/y	0.043 mm^2/y	−0.002%/y
LME model (IOP)					
P	–	0.64	0.44	0.78	0.81
Contralateral similarity					
ICC	–	0.79	0.54	0.78	0.53

LME, linear mixed effects model.

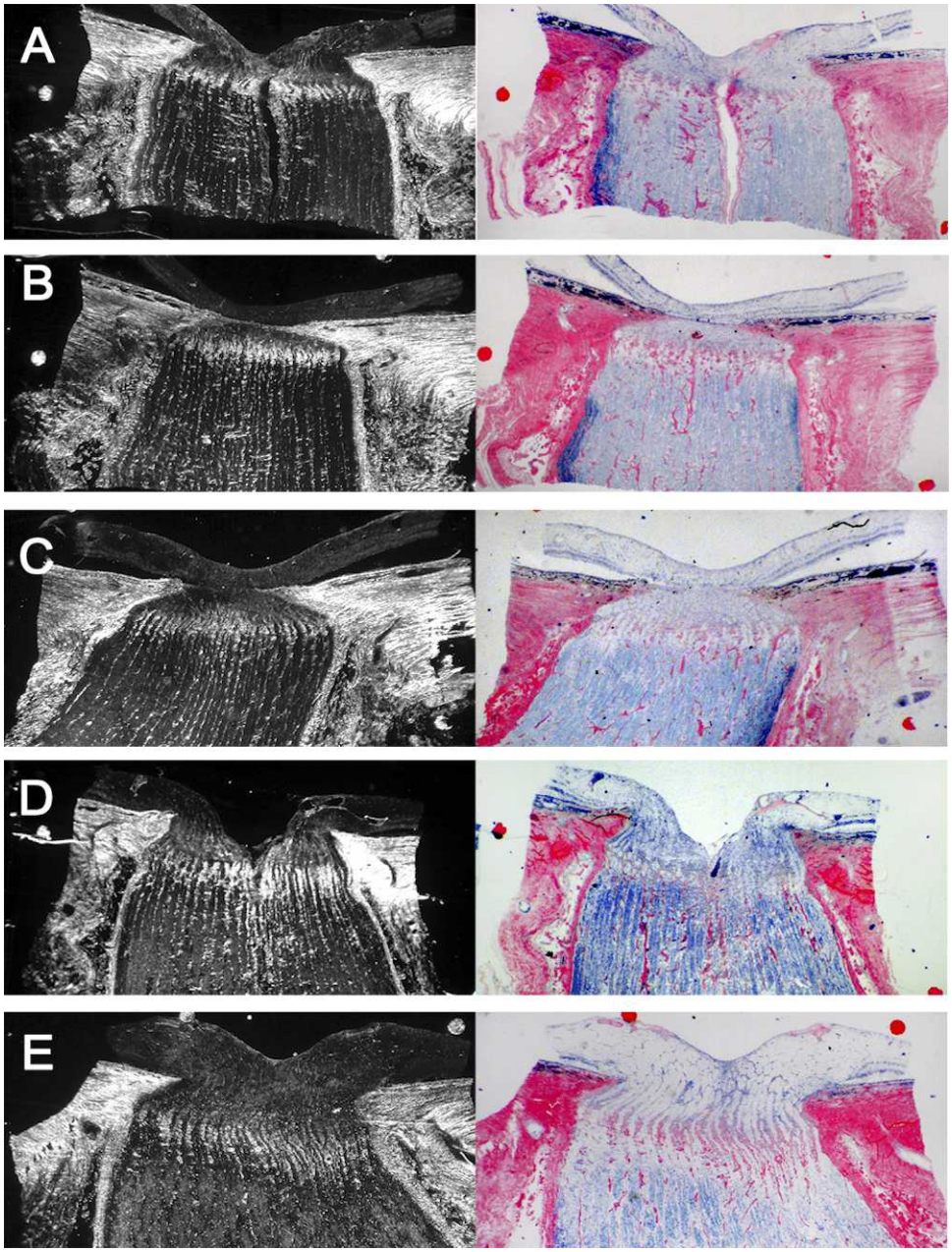

Figure 2. Dark-field (*left column*) and bright-field (*right column*) of ONH sections with LC insertion into the pia mater. The *top three rows* were acquired from sections of the eyes of a single donor (*right eye*: [**A**, **B**]; *left eye*: [**C**]). The two *bottom rows* come from different donors.

eye, and between 20% and 25% for the left eye. The association between age and the fraction of LC insertion into the pia was statistically significant when considering the higher values ($P = 0.0314$), but not when considering the lower ones ($P = 0.0972$, Fig. 5). Disregarding the measurements on the eyes of Donor 7 resulted in a stronger negative tendency for the model of the fraction of LC inserting into the pia mater with age, but with an associated increase in uncertainty in the estimate, such that the decrease with age was not statistically significant ($P = 0.0979$).

Discussion

Our goal was to measure the LC insertion into the sclera and pia mater in donor human eyes, and test the hypothesis that the LC insertion into the pia increases with aging. Two main findings arise from this work. First, the LC inserted universally into the pia mater and not just into the sclera, such that the fraction of LC inserting into the pia ranged from 2.2% to 29.6%. Second, the fraction of the LC inserting into the pia mater decreased with age ($P = 0.049$), caused by a nonsignificant decrease in the area of LC insertion into the pia ($P = 0.55$) and a nonsignificant increase in the total area of LC insertion ($P = 0.41$). We also found that the differences in measurements were smaller between fellow eyes than between unrelated eyes, consistent with previous studies of LC morphology.[2,15,25] None of the measures was associated with the level of IOP at fixation (P values 0.44–0.81).

To the best of our knowledge, this is the first study of the LC insertion in humans and its association with age. Our results are important because the LC is the principal site of neural tissue insult in glaucoma and, therefore, characterizing how

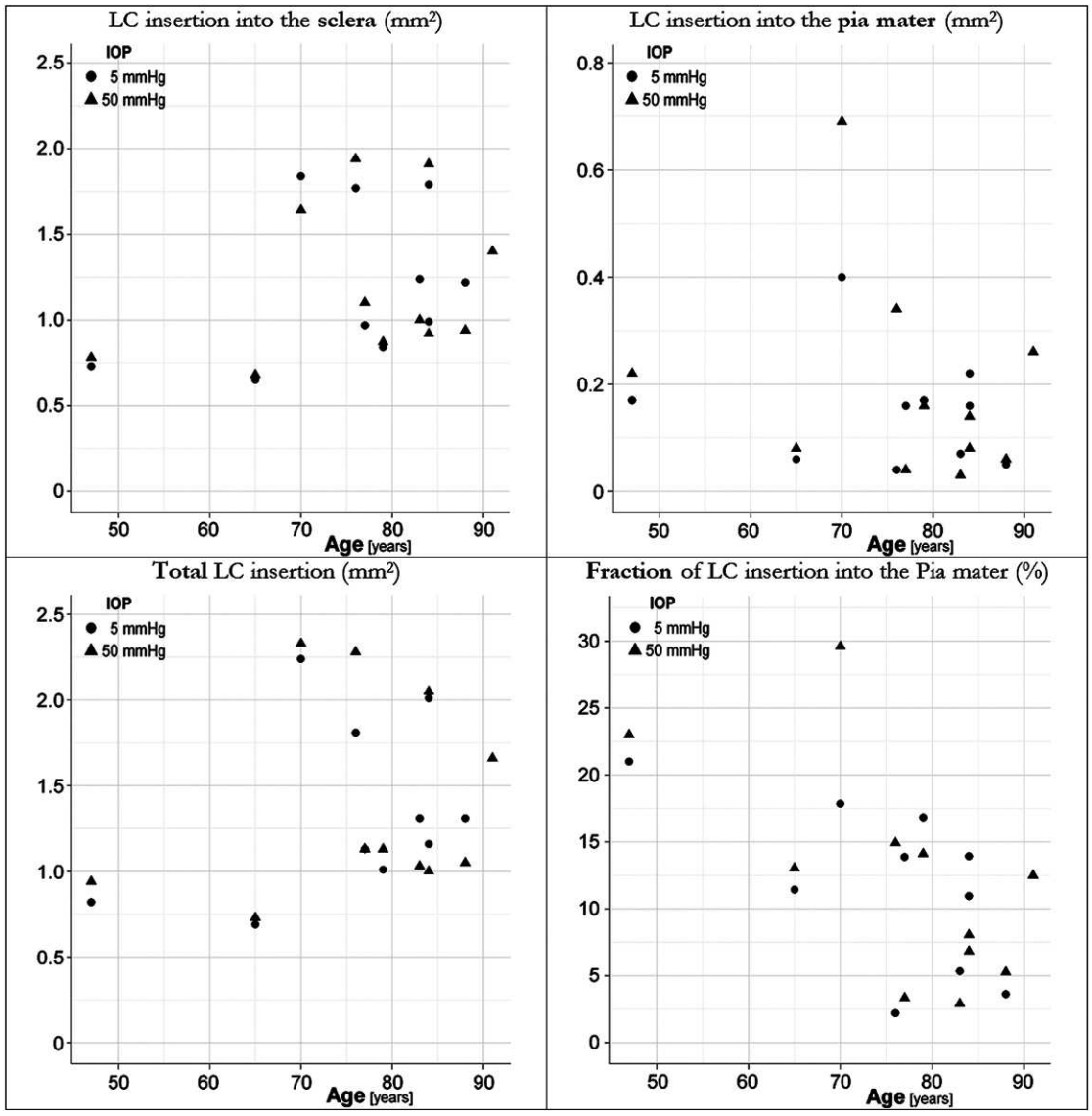

Figure 3. Scatter plots of the magnitude of LC insertion into the sclera (*top left*), the pia mater (*top right*), the total insertion (*bottom left*), and the fraction of LC inserting into the pia mater (*bottom right*).

this region changes with age is necessary to understand the normal and diseased eye. Although there is substantial variability between eyes, the aged ONH seems to increase in susceptibility to disease, and in particular to glaucoma.[26,27] Age is an independent risk factor for the prevalence[27] and progression of glaucomatous optic neuropathy,[28,29] even though IOP does not increase substantially with age.[30,31]

To our knowledge, insertion of the LC into the pia mater was first reported by us,[15] although it was proposed in 1947 by Wilckzek.[32] A recent report showed that the LCs of young ostensibly healthy monkeys did not insert into the pia mater.[16] The question thus arises as to whether in humans the extent of LC insertion into the pia mater increases with aging, or if this is a fundamental difference between species. The ability of the LC to remodel has been demonstrated in monkeys.[16,22,33] Eyes with induced hypertension had significantly more posterior LC than the contralateral control eye, sometimes posterior enough to be partially inserted into the pia mater. Analysis of the monkey LC structure by counting laminar beams found that, in the early stages of experimental glaucoma, the thickening of the LC is via the recruitment of retrolaminar tissue into the LC.[22] In humans, Jonas et al. reported some remarkable differences in peripapillary sclera morphology associated with high myopia, which may be due to remodeling.[8] Age, hypertension, and glaucoma have also been reported to result in variations in scleral characteristics, including thickness and mechanical properties.[34–37]

The periphery of the LC is important from vascular and biomechanical perspectives.[1,2,4,10,12,13,27,38,39] On the vascular side, much of the perfusion to the tissues within the LC, including the retinal ganglion cell axon bundles, is believed to be through microvessels and capillaries that enter the scleral canal from the periphery at the level of the LC insertion.[10,13] Additionally, the aged ONH is more likely to have a compromised blood supply,[2,10,12] which may affect sensitivity to IOP.[1,2,10,12,39] The forces and deformations transmitted to the LC by the load-bearing tissues surrounding the LC and scleral canal have a key role in the biomechanical robustness of the LC and its sensitivity to elevated IOP.[5,6,18,33,40–46] The biomechanical consequences of the LC inserting into the pia

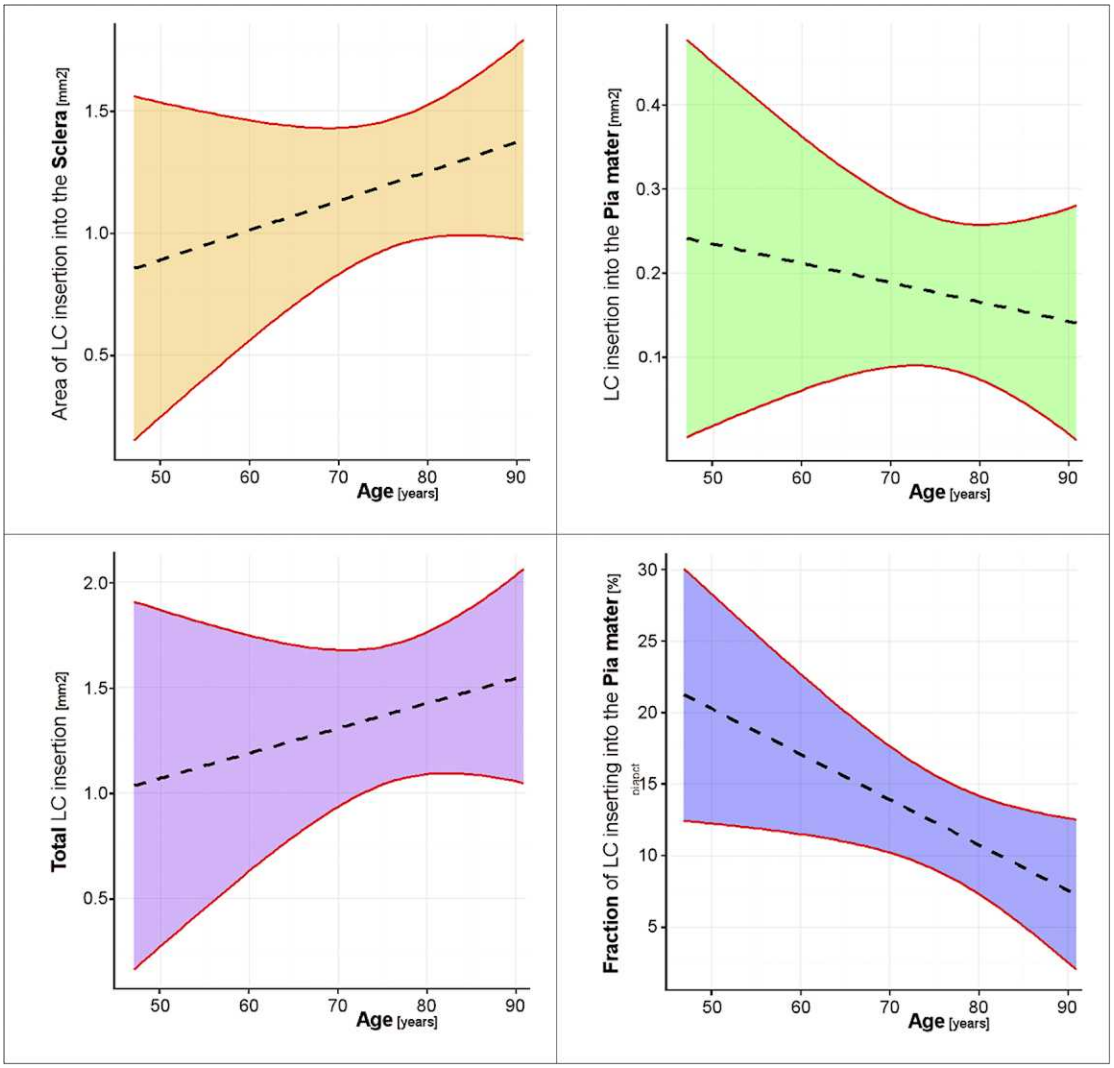

Figure 4. Fixed effects estimates based on the linear mixed effect models of the association between age and the LC insertion into the sclera (*top left*), the pia mater (*top right*), the total insertion (*bottom left*), and the fraction of LC inserting into the pia mater (*bottom right*). The *dashed line* is the best model estimate, whereas the 95% CI for the model is bounded by *red lines* and shaded in color. The CIs for the true regression line include all the lines that are plausible given the observed measurements – the slope/intercept values for these lines cannot be rejected. Lines that fall outside the CI bounds are not plausible – the slope/intercept values for these lines are rejected. Hence, CIs that allow a straight line with slope of zero cannot reject the null association. Only the fraction of LC inserting into the pia mater was statistically significant ($P = 0.0486$) with decreasing fraction of insertion with increasing age.

mater still are unclear, and likely depend on the mechanical properties of the pia mater, sclera, and retrolaminar neural tissue and septa.[4,5,33,40–42,47,48] Although the LC insertion into the pia mater was clear in the histology, it still is unknown whether the properties of the pia mater immediately adjacent to the LC are different from those of the pia mater elsewhere. The pia mater immediately adjacent to the LC often is thicker than the more distal pia.[15,46,49] In a study using parametric analysis and finite element modeling to determine the mechanical effects of IOP on the LC, we found that LCs that insert into the pia mater were more sensitive to the mechanical properties of the pia than LCs that only inserted into the sclera.[40] Understanding the full extent of the biomechanical consequences of the results we present is complicated by the multitude of factors affecting the ONH.[5,41,50–52] For example, several studies have shown that connective tissues, among them the monkey sclera, stiffen with aging.[34–37,53,54] Parametric studies suggest that stiffening of the LC, for example, could have very different consequences on the sensitivity of the LC to IOP depending on other parameters, including the LC position along the scleral canal.[5,51,52] These changes will compound with other known effects of aging on the tissues of the ONH, such as age-related optic nerve axon loss[4,47] and thickening of the basement membranes of the laminar capillary endothelial cells of the lamina trabeculae.[4]

Below, we discuss briefly the main advantages and limitations of our methodology compared to similar ones used to study the LC.[8,18,20,22,25,45,46,49,53,55]

Use of Multiple Images and Stains

Some characteristics of the ONH tissues were clearer in the dark-field images, while others were best identified in dual-stained bright-field images. The posterior surface of the LC, for example, often was clearest using the stain for myelin. To the best of our knowledge, no other study of LC morphology has used multiple stains and multiple image modalities to identify tissue boundaries. Segmenters were masked to the age and IOP

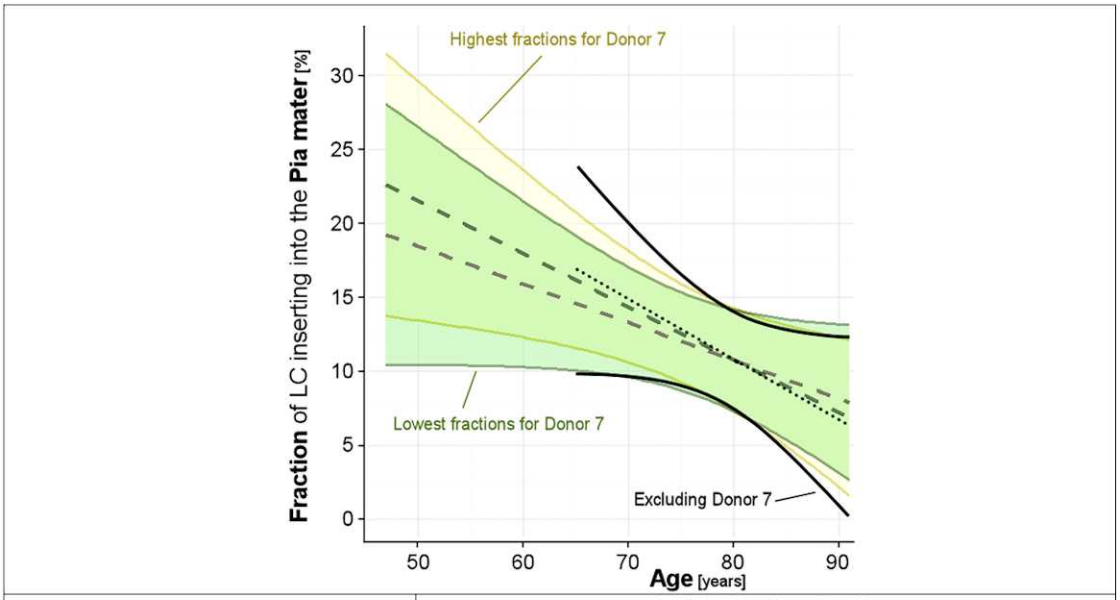

	LC insertion into the pia			
	Baseline (Figure 3)	Lowest fraction (Green region)	Highest fraction (Yellow region)	Removing Donor 7
% LC insertion into the pia (OD, OS)	23 %, 21 %	20 %, 18 %	25 %, 23 %	Removed
LME model (age)				
P	0.0486	0.0972	0.0314	0.0979
Slope	-0.317 %/y	-0.258 %/y	-0.357 %/y	-0.410 %/y
95% confidence interval. Min	-0.632 %/y	-0.573 %/y	-0.676 %/y	-0.914 %/y
Max	-0.002 %/y	0.057 %/y	-0.040 %/y	0.095 %/y

Figure 5. Analysis of results robustness. The plot shows the point estimates (*dashed lines*) and 95% CIs (*shaded regions*) for the fixed effects based on the linear mixed effects models obtained using two sets of values for the fraction of LC inserting into the pia mater. The decrease in fraction of LC inserting into the pia mater was statistically significant when using the highest fraction ($P = 0.0314$) and baseline ($P = 0.0486$), but not when using the lowest fraction ($P = 0.0972$). This is noticeable in the CIs in the table and graphically in the plot: the region shaded in *green* allows for a straight line with positive slope, whereas the region shaded in *yellow* does not. Traditionally once a threshold for significance has been defined (0.05 in this study) a fundamental but arbitrary distinction must be made between statistical models. Our intention with this illustration is to show that two models that appear sharply different, by nature of one being statistically significant and the other not statistically significant, actually represent similar associations between the parameters. For both statistical models the best estimate is that aging is associated with a decrease in the fraction of LC inserting into the pia mater. The key difference between the models is the likelihood of this hypothesis being due to chance. Since the threshold for significance is, in essence, arbitrary, we posit that it is more useful to interpret both models as useful even if slightly different.

of the eyes. On completion, the segmentations were checked for accuracy and consistency by two experienced segmenters (JGF and IAS). We believed that it is unlikely that the segmenters were biased because the eyes were segmented several years before the hypothesis in this study was formulated.

Measurement in Multiple Sections and 3D

The problems associated with measurements on single sections in histologic analysis have been discussed elsewhere.[15,18,56] One issue is the probability of missing small or relatively infrequent occurrences, such as the LC insertion into the pia mater. All measurements were taken using multiple sections. In addition, our histology used JB-4 plastic with carefully incorporated fiducial markers, subsequently used to unwarp the individual sections.

Iterative Checking

We used an iterative approach in which the geometric integrity of the structure was evaluated and refined until a series of requirements was satisfied. This ensured that all features of the reconstructions, and hence the measurements based on them, were consistent with each other. Without an iterative process there is little opportunity to compensate for factors that could affect measurements.

We recognize that delineation of tissues can be ambiguous. Thus, we conducted an analysis on the robustness of the results and conclusions by considering alternative tissue delineations and measurements. The baseline case is the most appropriate because it is the one that satisfied all the requirements in our iterative process. Using the alternate segmentations resulted in slight changes in the measurements, with a consequent range in the significance of the statistical models (P = [0.03, 0.10]). Even though this range extends above the threshold of 0.05 for statistical significance, plotting of the model estimates and the associated confidence intervals (CIs) shows that these differences are small from a practical perspective. Hence, our conclusion that the fraction of LC inserting into the pia mater does not increase with age is robust to variability in the segmentations. The alternate segmentations and measurements were extreme cases considered to test the robustness of the results. Our intention was to acknowledge that there always will be some degree of arbitrariness in the manual identification of the boundaries

between tissues. The variability in the fraction of LC insertion into the pia mater resulting from the use of alternate segmentations is not an adequate measurement of error or uncertainty in the measurements of this quantity in other eyes. Disregarding the measurements on the eyes of Donor 7 also resulted in changes in the model of the fraction of LC insertion into the pia as a function of age. Interestingly, while the estimate was more strongly negative, the widening of the CIs meant that the model was not statistically significant ($P = 0.10$). Note that we believe that there is no sound reason to exclude the measurements from the eyes of Donor 7. We did this with the sole intention of demonstrating that, for practical purposes, the main conclusions of this work did not depend on these measurements. On the statistical analysis, it also is worth noting that the results presented do not include a Bonferroni correction. A correction would have reduced the threshold for statistical significance, but our analysis has shown that the conclusions are robust to the choice of threshold, which ultimately is arbitrary. Further, even among statisticians there is no formal consensus for when Bonferroni procedures should be used.[57] Thus, we believe that, irrespective of a correction, it is valid to conclude that there is no evidence that the fraction of LC inserting into the pia mater increases with age, and that the model estimates suggest a decrease with age, albeit with substantial uncertainty.

Figures 1 and 2 present six sections of the optic nerve head showing lamina insertion into the pia mater. In some of these cases the insertion is clear in the dark-field and bright-field images. In other cases it is difficult to distinguish. We realize that it is worth considering why we have been able to present lamina insertion into the pia mater that other studies of lamina anatomy have not identified. While it is impossible to know for certain, several factors may help explain this. First, the small fraction of insertion into the pia mater (2.2%–29.6%) means that in many eyes the pia insertion is easy to miss. For sections with only a minimal insertion into the pia it seems plausible that someone delineating the lamina cribrosa may not notice this insertion, especially if they anticipate that the lamina may insert only into the sclera. Second, we delineated the tissues based on multiple images and stains. Third, we embedded the fixed tissue in JB-4 plastic before sectioning. This is a less common, relatively difficult technique, compared to the more usual paraffin blocking. The reason for using JB-4 was to maintain a more accurate anatomic structure. We combined this with the use of fiducial markers and image unwarping. Fourth, we delineated 3D stacks of images, not single sections. This helps in identifying features that occur in a small fraction of the lamina periphery, and allowed use of adjacent sections and the iterative checking procedure to obtain more reliable measurements. Often the lamina insertion into the pia mater appeared in consecutive sections, reducing the likelihood of misidentification. The images used for reconstruction were selected as the best examples out of a larger set of sections, improving overall quality, again reducing the likelihood of artifacts. We also would like to point out that since our presentation of the first evidence for pial insertion,[15] others have confirmed the phenomenon in monkeys and humans,[16] using different techniques. They have even reported full insertion of the lamina into the pia (i.e., no insertion into the sclera in that region). We believe that the lamina insertion into the pia mater may have been noticed long ago if more attention had been paid to the tissues immediately adjacent to the lamina. We recently showed an image captured by Quigley et al. from more than two decades ago where pial insertion of the lamina is visible.[58] More recently, the interest in the tissues adjacent to the optic nerve head has increased, leading to improved knowledge of this region.[8,59–62] Nevertheless, we acknowledge that it is possible that other imaging techniques or alternate definitions of what constitutes the laminar region may lead to different understandings of the morphology of the tissues of the optic nerve head, including the lamina cribrosa insertion.

Limitations related to the use of serial histologic sections have been discussed elsewhere.[1,15,17,40] While we acknowledge that the effects of these artifacts can be substantial, we believe that measurements of the relative lengths of the boundaries between tissues are insensitive to the effects of warping and shrinkage compared with absolute measures of length or shape, and therefore that our main conclusion, namely that the fraction of LC inserting into the pia mater decreases with age, is not due to these artifacts. This was assisted further by the use of JB-4 plastic with embedded fiducial markers. The eyes were fixed at IOPs of 5 or 50 mm Hg for a separate study of the biomechanical effects of IOP on the ONH, the results of which we have reported elsewhere.[6,15,40] We found that variability in ONH morphology, including LC insertion, often was greater than the differences due to IOP. It seems reasonable to expect that the fraction of LC inserting into the pia mater is insensitive to fixation pressure, consistent with our finding of no association with IOP.

Our study relied on the use of postmortem eyes and, although we enforced strict controls, we cannot exclude the possibility that degenerative changes after death could have altered some aspects of ONH anatomy. Since postmortem eyes tend to be from older subjects, there may be characteristics in the LC insertion in younger eyes that we have not accounted for. Also, postmortem data are, by definition, cross-sectional and longitudinal characterization of the progression of LC insertion into the pia is necessary to determine if there is a process of LC migration in the human that parallels that reported in the monkey.[16] This soon may be possible with the development of imaging tools and techniques, such as longer wavelength spectral domain optical coherence tomography (SD-OCT) or enhanced depth OCT (ED-OCT).[55,63–65] Still, it remains to be demonstrated whether these techniques enable imaging of the posterior LC insertion, as it generally is deep and obscured by the overlying sclera.[15,17]

Although we analyzed twice as many eyes as in our previous morphometric analysis, and more than most 3D morphometric studies of the LC, the number still is modest. The main reason for this was the time required for tissue processing, image analysis and model reconstruction, which again may be overcome by the development of advanced imaging methods.[20,21,55,65–67] In summary, to our knowledge we present the first findings to suggest that LC insertion into the pia mater is a common phenomenon in middle-aged and older human eyes, and that changes in the LC insertion may be part of the normal aging process. Insertion of the LC into the pia mater may have biomechanical and vascular implications that should be investigated further because they could be important for understanding the risk factors for and pathophysiology of glaucomatous optic neuropathy.

References

1. Sigal IA, Ethier CR. Biomechanics of the optic nerve head. *Exp Eye Res*. 2009;88:799–807.
2. Burgoyne CF, Downs JC, Bellezza AJ, Suh JK, Hart RT. The optic nerve head as a biomechanical structure: a new paradigm for understanding the role of IOP-related stress and strain in the pathophysiology of glaucomatous optic nerve head damage. *Prog Retin Eye Res*. 2005;24:39–73.
3. Quigley HA, Flower RW, Addicks EM, McLeod DS. The mechanism of optic nerve damage in experimental acute intraocular pressure elevation. *Invest Ophthalmol Vis Sci*. 1980;19:505–517.

4. Hernandez MR. The optic nerve head in glaucoma: role of astrocytes in tissue remodeling. *Prog Retin Eye Res*. 2000;19: 297–321.
5. Sigal IA. Interactions between geometry and mechanical properties on the optic nerve head. *Invest Ophthalmol Vis Sci*. 2009;50:2785–2795.
6. Sigal IA, Flanagan JG, Tertinegg I, Ethier CR. Predicted extension, compression and shearing of optic nerve head tissues. *Exp Eye Res*. 2007;85:312–322.
7. Bellezza AJ. *Biomechanical Properties of the Normal and Early Glaucomatous Optic Nerve Head: An Experimental and Computational Study Using the Monkey Model*. Department of Biomedical Engineering. New Orleans, LA: Tulane University; 2002. Thesis.
8. Jonas JB, Jonas SB, Jonas RA, Holbach L, Panda-Jonas S. Histology of the parapapillary region in high myopia. *Am J Ophthalmol*. 2011;152:1021–1029.
9. Tektas OY, Lutjen-Drecoll E, Scholz M. Qualitative and quantitative morphologic changes in the vasculature and extracellular matrix of the prelaminar optic nerve head in eyes with POAG. *Invest Ophthalmol Vis Sci*. 2010;51:5083–5091.
10. Mackenzie PJ, Cioffi GA. Vascular anatomy of the optic nerve head. *Can J Ophthalmol*. 2008;43:308–312.
11. Jonas JB, Jonas SB. Histomorphometry of the circular peripapillary arterial ring of Zinn-Haller in normal eyes and eyes with secondary angle-closure glaucoma. *Acta Ophthalmol*. 2010;88:e317–e322.
12. Burgoyne CF. A biomechanical paradigm for axonal insult within the optic nerve head in aging and glaucoma. *Exp Eye Res*. 2011;93:120–132.
13. Hayreh SS. The blood supply of the optic nerve head and the evaluation of it – myth and reality. *Prog Retin Eye Res*. 2001; 20:563–593.
14. Hiraoka M, Inoue K, Ninomiya T, Takada M. Ischaemia in the Zinn-Haller circle and glaucomatous optic neuropathy in macaque monkeys. *Br J Ophthalmol*. 2012;96:597–603.
15. Sigal IA, Flanagan JG, Tertinegg I, Ethier CR. 3D morphometry of the human optic nerve head. *Exp Eye Res*. 2010;90:70–80.
16. Yang H, Williams G, Downs JC, et al. Posterior (outward) migration of the lamina cribrosa and early cupping in monkey experimental glaucoma. *Invest Ophthalmol Vis Sci*. 2011;52: 7109–7121.
17. Sigal IA, Flanagan JG, Tertinegg I, Ethier CR. Reconstruction of human optic nerve heads for finite element modeling. *Technol Health Care*. 2005;13:313–329.
18. Yan DB, Flanagan JG, Farra T, Trope GE, Ethier CR. Study of regional deformation of the optic nerve head using scanning laser tomography. *Curr Eye Res*. 1998;17:903–916.
19. Quigley HA, Addicks EM. Regional differences in the structure of the lamina cribrosa and their relation to glaucomatous optic nerve damage. *Arch Ophthalmol*. 1981;99:137–143.
20. Winkler M, Jester B, Nien-Shy C, et al. High resolution three-dimensional reconstruction of the collagenous matrix of the human optic nerve head. *Brain Res Bull*. 2010;81:339–348.
21. Brown DJ, Morishige N, Neekhra A, Minckler DS, Jester JV. Application of second harmonic imaging microscopy to assess structural changes in optic nerve head structure ex vivo. *J Biomed Opt*. 2007;12:024029.
22. Roberts MD, Grau V, Grimm J, et al. Remodeling of the connective tissue microarchitecture of the lamina cribrosa in early experimental glaucoma. *Invest Ophthalmol Vis Sci*. 2009;50:681–690.
23. Team RDCR: *A Language and Environment for Statistical Computing*. Vienna, Austria: R Foundation for Statistical Computing; 2011.
24. Bates D, Mächler M, Bolker B. lme4: linear mixed-effects models using S4 classes. *R package version 0.999375-42*. 2011. Available at http://cran.r-project.org/web/packages/lme4/index.html. Accessed January 20, 2012.
25. Yang H, Downs JC, Burgoyne CF. Physiologic intereye differences in monkey optic nerve head architecture and their relation to changes in early experimental glaucoma. *Invest Ophthalmol Vis Sci*. 2009;50:224–234.
26. Suzuki Y, Iwase A, Araie M, et al. Risk factors for open-angle glaucoma in a Japanese population: the Tajimi Study. *Ophthalmology*. 2006;113:1613–1617.
27. Quigley HA. Glaucoma. *Lancet*. 2011;377:1367–1377.
28. Gordon MO, Beiser JA, Brandt JD, et al. The Ocular Hypertension Treatment Study: baseline factors that predict the onset of primary open-angle glaucoma. *Arch Ophthalmol*. 2002;120:714–720; discussion 829–830.
29. Heijl A, Leske MC, Bengtsson B, Hussein M. Measuring visual field progression in the Early Manifest Glaucoma Trial. *Acta Ophthalmol Scand*. 2003;81:286–293.
30. Leskea MC, Heijl A, Hyman L, Bengtsson B, Komaroff E. Factors for progression and glaucoma treatment: the Early Manifest Glaucoma Trial. *Curr Opin Ophthalmol*. 2004;15: 102–106.
31. Rochtchina E, Mitchell P, Wang JJ. Relationship between age and intraocular pressure: the Blue Mountains Eye Study. *Clin Experiment Ophthalmol*. 2002;30:173–175.
32. Wilczek M. The lamina cribrosa and its nature. *Br J Ophthalmol*. 1947;31:551–565.
33. Roberts MD, Sigal IA, Liang Y, Burgoyne CF, Downs JC. Changes in the biomechanical response of the optic nerve head in early experimental glaucoma. *Invest Ophthalmol Vis Sci*. 2010;51:5675–5684.
34. Coudrillier B, Tian J, Alexander S, Myers KM, Quigley HA, Nguyen TD. Mechanical response of the human posterior sclera: age and glaucoma related changes measured using inflation testing. *Invest Ophthalmol Vis Sci*. 2012;53:1714–1728.
35. Girard MJ, Suh JK, Bottlang M, Burgoyne CF, Downs JC. Scleral biomechanics in the aging monkey eye. *Invest Ophthalmol Vis Sci*. 2009;50:5226–5237.
36. Girard MJ, Suh JK, Bottlang M, Burgoyne CF, Downs JC. Biomechanical changes in the sclera of monkey eyes exposed to chronic IOP elevations. *Invest Ophthalmol Vis Sci*. 2011;52: 5656–5669.
37. Yan D, McPheeters S, Johnson G, Utzinger U, Vande Geest JP. Microstructural differences in the human posterior sclera as a function of age and race. *Invest Ophthalmol Vis Sci*. 2011;52: 821–829.
38. Liang Y, Fortune B, Cull G, Cioffi GA, Wang L. Quantification of dynamic blood flow autoregulation in optic nerve head of rhesus monkeys. *Exp Eye Res*. 2010;90:203–209.
39. Quigley HA. Glaucoma: macrocosm to microcosm the Friedenwald lecture. *Invest Ophthalmol Vis Sci*. 2005;46: 2662–2670.
40. Sigal IA, Flanagan JG, Tertinegg I, Ethier CR. Modeling individual-specific human optic nerve head biomechanics. Part I: IOP-induced deformations and influence of geometry. *Biomech Model Mechanobiol*. 2009;8:85–98.
41. Sigal IA, Flanagan JG, Ethier CR. Interactions between factors influencing optic nerve head biomechanics. Presented at the American Society of Mechanical Engineers (ASME) Summer Bioengineering Conference. Keystone, CO; 2007.
42. Roberts MD, Liang Y, Sigal IA, et al. Correlation between local stress and strain and lamina cribrosa connective tissue volume fraction in normal monkey eyes. *Invest Ophthalmol Vis Sci*. 2010;51:295–307.
43. Strouthidis NG, Fortune B, Yang H, Sigal IA, Burgoyne CF. The effect of acute intraocular pressure elevation on the monkey optic nerve head as detected by spectral domain optical

coherence tomography. *Invest Ophthalmol Vis Sci*. 2011;52:9431–9437.

44. Levy NS, Crapps EE. Displacement of optic nerve head in response to short-term intraocular pressure elevation in human eyes. *Arch Ophthalmol*. 1984;102:782–786.
45. Fatehee N, Yu PK, Morgan WH, Cringle SJ, Yu DY. The impact of acutely elevated intraocular pressure on the porcine optic nerve head. *Invest Ophthalmol Vis Sci*. 2011;52:6192–6198.
46. Morgan WH, Chauhan BC, Yu DY, Cringle SJ, Alder VA, House PH. Optic disc movement with variations in intraocular and cerebrospinal fluid pressure. *Invest Ophthalmol Vis Sci*. 2002;43:3236–3242.
47. Hernandez MR, Luo XX, Andrzejewska W, Neufeld AH. Age-related changes in the extracellular matrix of the human optic nerve head. *Am J Ophthalmol*. 1989;107:476–484.
48. Grytz R, Meschke G, Jonas JB. The collagen fibril architecture in the lamina cribrosa and peripapillary sclera predicted by a computational remodeling approach. *Biomech Model Mechanobiol*. 2011;10:371–382.
49. Oyama T, Abe H, Ushiki T. The connective tissue and glial framework in the optic nerve head of the normal human eye: light and scanning electron microscopic studies. *Arch Histol Cytol*. 2006;69:341–356.
50. Sigal IA. An applet to estimate the IOP-induced stress and strain within the optic nerve head. *Invest Ophthalmol Vis Sci*. 2011;52:5497–5506.
51. Sigal IA, Yang H, Roberts MD, Burgoyne CF, Downs JC. IOP-induced lamina cribrosa displacement and scleral canal expansion: an analysis of factor interactions using parameterized eye-specific models. *Invest Ophthalmol Vis Sci*. 2011;52:1896–1907.
52. Sigal IA, Yang H, Roberts MD, et al. IOP-induced lamina cribrosa deformation and scleral canal expansion: independent or related? *Invest Ophthalmol Vis Sci*. 2011;52:9023–9032.
53. Albon J, Farrant S, Akhtar S, et al. Connective tissue structure of the tree shrew optic nerve and associated ageing changes. *Invest Ophthalmol Vis Sci*. 2007;48:2134–2144.
54. Albon J, Purslow PP, Karwatowski WS, Easty DL. Age related compliance of the lamina cribrosa in human eyes. *Br J Ophthalmol*. 2000;84:318–323.
55. Park SC, De Moraes CG, Teng CC, Tello C, Liebmann JM, Ritch R. Enhanced depth imaging optical coherence tomography of deep optic nerve complex structures in glaucoma. *Ophthalmology*. 2011;119:3–9.
56. Jonas JB, Berenshtein E, Holbach L. Anatomic relationship between lamina cribrosa, intraocular space, and cerebrospinal fluid space. *Invest Ophthalmol Vis Sci*. 2003;44:5189–5195.
57. Nakagawa S. A farewell to Bonferroni: the problems of low statistical power and publication bias. *Behav Ecol*. 2004;15:1044–1045.
58. Crawford Downs J, Roberts MD, Sigal IA. Glaucomatous cupping of the lamina cribrosa: a review of the evidence for active progressive remodeling as a mechanism. *Exp Eye Res*. 2011;93:133–140.
59. Norman RE, Flanagan JG, Rausch SM, et al. Dimensions of the human sclera: thickness measurement and regional changes with axial length. *Exp Eye Res*. 2010;90:277–284.
60. Yang H, Downs JC, Girkin C, et al. 3-D histomorphometry of the normal and early glaucomatous monkey optic nerve head: lamina cribrosa and peripapillary scleral position and thickness. *Invest Ophthalmol Vis Sci*. 2007;48:4597–4607.
61. Balaratnasingam C, Morgan WH, Johnstone V, Pandav SS, Cringle SJ, Yu DY. Histomorphometric measurements in human and dog optic nerve and an estimation of optic nerve pressure gradients in human. *Exp Eye Res*. 2009;89:618–628.
62. Jonas JB, Hayreh SS, Tao Y. Central corneal thickness and thickness of the lamina cribrosa and peripapillary sclera in monkeys. *Arch Ophthalmol*. 2009;127:1395–1396.
63. Kiumehr S, Park SC, Dorairaj S, et al. In vivo evaluation of focal lamina cribrosa defects in glaucoma. *Arch Ophthalmol*. 2012;130:552–559.
64. Park SC, Kiumehr S, Teng CC, Tello C, Liebmann JM, Ritch R. Horizontal central ridge of the lamina cribrosa and regional differences in laminar insertion in normal subjects. *Invest Ophthalmol Vis Sci*. 2012;53:1610–1616.
65. Girard MJ, Strouthidis NG, Ethier CR, Mari JM. Shadow removal and contrast enhancement in optical coherence tomography images of the human optic nerve head. *Invest Ophthalmol Vis Sci*. 2011;52:7738–7748.
66. Strouthidis NG, Fortune B, Yang H, Sigal IA, Burgoyne CF. Longitudinal change detected by spectral domain optical coherence tomography in the optic nerve head and peripapillary retina in experimental glaucoma. *Invest Ophthalmol Vis Sci*. 2011;52:1206–1219.
67. Kagemann L, Ishikawa H, Wollstein G, et al. Ultrahigh-resolution spectral domain optical coherence tomography imaging of the lamina cribrosa. *Ophthalmic Surg Lasers Imaging*. 2008;39:S126–S131.